

1           **Persistence of populations facing climate velocity and**  
2           **harvest**

3           Emma Fuller<sup>1</sup>, Eleanor Brush<sup>2</sup>, Malin L. Pinsky<sup>1,3</sup>

4           (1): Department of Ecology and Evolutionary Biology, Princeton University, Princeton, New  
5           Jersey 08544 USA

6           (2): Program in Quantitative and Computational Biology, Princeton University, Princeton, New  
7           Jersey 08544 USA

8           (3): Department of Ecology, Evolution and Natural Resources, Rutgers University, New  
9           Brunswick, New Jersey 08901 USA

10    **Abstract**

11    Many species are expected to shift their geographic distribution as climates change, and yet  
12    climate change is only one of a suite of stressors that species face. Species that might, in theory,  
13    be able to shift rapidly enough to keep up with climate velocity (the rate and direction that  
14    isotherms move across the landscape) may not in actuality be able to do so when facing the  
15    cumulative impacts of multiple stressors. However, despite empirical reports of substantial  
16    interactions between climate change and other stressors, we often lack a mechanistic  
17    understanding of these interactions. Here, we develop and analyze a spatial population dynamics  
18    model to explore the cumulative impacts of climate with another dominant stressor in the ocean  
19    and on land: harvest. Our results delineate the conditions under which harvesting and climate  
20    velocity can together drive populations extinct even when neither stressor would do so in  
21    isolation. We find that critical rates of harvest and climate velocity depend on the growth rate  
22    and dispersal kernel of the population, as well as the magnitude of the other stressor. We also  
23    find that, in our model, the declines in biomass caused by climate velocity and harvest are at  
24    most slightly greater than the sum of the declines caused by either stressor individually (e.g.,  
25    approximately additive) and that threshold harvest rules can be effective management tools to  
26    mitigate the interaction between the two stressors.

27    **Keywords:** Climate change, fishing, integrodifference model, synergy, multiple disturbances,  
28    cumulative impacts

29 **Introduction**

30 There are many stressors that can disturb an ecosystem, and ecologists have long quantified the  
31 consequences of individual perturbations (Wilcove et al. 1998). Less work, however, has been  
32 done to measure the effects of multiple stressors and the interactions between them (Travis 2003;  
33 Crain et al. 2008; Darling and Côté 2008). If disturbances interact synergistically, a perturbation  
34 that has little effect when occurring alone may amplify the disturbance caused by a coincident  
35 perturbation (Crain et al. 2008; Darling and Côté 2008; Nye et al. 2013; Gurevitch et al. 2000).  
36 In the most worrying cases, interactions among multiple stressors could drive a population  
37 extinct even though assessments of individual impacts would suggest otherwise (e.g., Pelletier et  
38 al. 2006; Travis 2003). Because disturbances rarely occur in isolation, measuring the effects of  
39 multiple disturbances provides a better understanding of likely impacts to an ecosystem (Doak  
40 and Morris 2010; Fordham et al. 2013; Folt et al. 1999).

41 Climate change and harvesting, two of the largest anthropogenic impacts for both marine and  
42 terrestrial species (Milner-Gulland and Bennet 2003; Sekercioglu et al. 2008; Halpern et al.  
43 2008), provide an important example of ecological disturbances occurring in unison. One effect  
44 of climate change is that isotherms move across a landscape with a rate and direction referred to  
45 as climate velocity (Loarie et al. 2009; Burrows et al. 2011). Marine and terrestrial population  
46 distributions shift in response to climate change (Perry et al. 2005; Chen et al. 2011), and there is  
47 evidence that climate velocities can successfully explain these shifts (Pinsky et al. 2013).

48 Many of these shifting species, however, are also subject to harvesting or fishing (Wilcove et al.  
49 1998; Sala 2000; Worm et al. 2009), such that interactions between the two stressors are  
50 possible. For example, empirical data suggest that Atlantic croaker populations move poleward

51 with warming temperatures, but do so less when heavily fished (Hare et al. 2010). In addition,  
52 climate and fishing both appear to have influenced the distribution of North Sea cod over the past  
53 century (Engelhard et al. 2014). While not specifically addressing range shifts and harvest  
54 together, synergistic interactions between warming temperatures and harvesting have been  
55 identified in microcosm experiments (Mora et al. 2007), observations suggest that species follow  
56 warming temperatures more effectively in protected areas than in unprotected land (Thomas et  
57 al. 2012), and a number of studies conclude that harvest increases the sensitivity of populations  
58 to climate variability (Anderson et al. 2008; Botsford et al. 2011; Shelton et al. 2011; Planque et  
59 al. 2011). Taken together, this work underscores the importance of understanding in greater  
60 mechanistic detail how climate velocity and harvesting interact. Models provide a useful tool in  
61 this situation for building our intuition.

62 A common approach to modeling climate impacts has been to use bioclimatic-envelope models  
63 (also known as species distribution models). These statistical models typically correlate  
64 presence-absence or abundance data with biophysical characteristics to predict how species'  
65 ranges will differ under climate change (Elith et al. 2006; Guisan and Thuiller 2005; Guisan and  
66 Zimmermann 2000). Despite these models' widespread adoption, many authors have criticized  
67 bioclimatic-envelope models as oversimplified because they lack dispersal, reproduction, species  
68 interaction, and other processes important for population dynamics (Kearney and Porter 2009;  
69 Zarnetske et al. 2012; Robinson et al. 2011).

70 Recent work on range shifts has addressed some of these gaps by explicitly including dispersal  
71 and reproduction in models for species distributions under climate change (Berestycki et al.  
72 2009; Zhou and Kot 2011). In these latter models, the region in which a population can survive  
73 (e.g., the region of suitable temperatures) is shifting in space, and a population can only survive

74 if it disperses to and grows in newly suitable habitat at a sufficient rate. Related models have  
75 been applied to study population persistence in advective environments (Byers and Pringle  
76 2006). However, even these more mechanistic models only address one disturbance: climate-  
77 driven range shifts.

78 Here, we focus on a relatively simple ecological model that captures the dominant processes  
79 (reproduction, dispersal, and population growth) underlying climate-driven range shifts and  
80 population responses to harvesting pressure. We built this model originally for marine species;  
81 but because of its mathematical generality, it could also apply to any species with distinct growth  
82 and dispersal stages (e.g., plants, trees, and many insects). We derive the harvesting rate and  
83 climate velocity that drive populations extinct, and explore the combined demographic effects of  
84 these stressors. We show that the declines in biomass caused by climate-driven range shifts and  
85 harvest are at most only slightly greater than the sum of the declines caused by either stressor  
86 individually. In other words, the cumulative impacts are approximately additive. We also  
87 examine the efficacy of two different types of management strategies: threshold harvesting rules  
88 and protected areas. Protected areas are often recommended for conservation of biodiversity and  
89 improved yield from harvest (Pimm et al. 2001, Gaines et al. 2010b, Watson et al. 2011), and  
90 previous work has suggested protected areas can be a key form of climate insurance that  
91 provides stepping stones to help species keep up with a changing environment (Thomas et al.  
92 2012; Hannah et al. 2007). We find that protected areas can help a species persist with higher  
93 harvesting pressure and can increase the maximum climate velocity a harvested species can  
94 survive. We also find that threshold-harvesting rules have a fundamentally different effect and  
95 largely remove the strongest interactions between harvesting rates and climate velocity.

96 **Methods**

97 We model the dynamics of populations along a one-dimensional line of longitude, similar to  
98 Zhou and Kot (2011). Individuals in the population can only reproduce within a defined segment  
99 of the environment (hereafter simply “patch”), which represents the range of thermally suitable  
100 conditions for the population. The patch shifts at a fixed rate towards the poles (i.e., at the rate of  
101 climate velocity), and offspring disperse away from their parents according to a dispersal kernel.  
102 In its basic form, harvest removes a constant fraction of the local population density from each  
103 point along the coastline.

104 To investigate the model, we first analytically determine the combinations of harvesting rate and  
105 climate velocity that drive the population extinct (hereafter the critical harvesting rate and critical  
106 climate velocity), and then measure their interaction by calculating the decrease in biomass  
107 caused by the stressors both individually and together. We then add threshold harvesting rules  
108 and protected areas in numerical simulations to determine how these management strategies  
109 affect population persistence and biomass.

110 **The Model**

111 The above verbal description is represented well by integro-difference models, which have been  
112 used extensively for spatial population dynamics problems with discrete time (e.g., discrete  
113 growth and dispersal stages) and continuous space (Kot and Schaffer 1996; Van Kirk and Lewis  
114 1997; Lockwood et al. 2002; Zhou and Kot 2010). More specifically, if  $n_t(x)$  is the number of  
115 individuals settling after dispersal at position  $x$  and time  $t$ , then the number of individuals in the  
116 next generation is given by

$$n_{t+1}(x) = \int_{-\frac{L}{2}+ct}^{\frac{L}{2}+ct} k(x-y)R_0g(f(n_t(y))) dy, \quad (1)$$

117 where  $f(n)$  is a recruitment function describing the number of offspring that settle and survive in  
 118 juvenile population of size  $n$ ,  $g(n)$  is a function describing the number of adults that remain after  
 119 harvesting given local density  $n$ ,  $R_0$  is the intrinsic growth rate of the population (e.g., number of  
 120 offspring per adult),  $k(x - y)$ , is a dispersal kernel giving the probability of an offspring  
 121 traveling from position  $y$  to position  $x$ . The model integrates over all reproduction that occurs  
 122 within the suitable thermal habitat patch, where  $L$  is the length of the patch and  $c$  is the rate at  
 123 which the patch shifts across space (the rate of climate velocity). In other words, the center of the  
 124 patch at time  $t$  will be at location  $ct$ , and so the upper and lower bounds of the patch will be  
 125 found at  $ct + L/2$  and  $ct - L/2$ , respectively.

126 Initially, we use  $g(n) = n - hn$  as our function for those surviving harvesting, where  $h$  is the  
 127 proportion of the population harvested. This model envisions that harvest removes a constant  
 128 fraction from each location  $x$ , as could be expected from an even distribution of harvesters across  
 129 space.

130 We also used a Beverton-Holt stock-recruitment function to describe the settlement and survival  
 131 of offspring  $f(n)$  accounting for density dependent competition and mortality:

$$f(n) = \frac{n}{1 + \left(\frac{R_0-1}{K}\right)n} \quad (2)$$

132 As before,  $R_0$  is the intrinsic growth rate, while  $K$  is the carrying capacity at a given point in  
 133 space, which we assume to be constant (see Table 1 for a full description of parameters and

134 functions). If  $n = K$ , then  $f(n) = \frac{n}{R_0}$  and when those surviving offspring reproduce at rate  $R_0$  the  
 135 population will remain at  $K$ . As shown in Appendix A.1, the precise forms of  $g(n)$  and  $f(n)$  are  
 136 not important to the persistence of the population, which instead depends only on  $g'(0)$  and  
 137  $f'(0)$ . The full functional forms, however, are important for equilibrium population levels.

138 Analyzing this kind of model becomes easier if the dispersal kernel is separable into its  
 139 dependence on sources and destinations of larvae, that is if there are functions  $a_i, b_i$  such that  
 140  $k(x - y) = \sum_{i=1}^{\infty} a_i(x)b_i(y)$  (see Appendix A.2 for further details). In the analyses presented  
 141 below, we used a Gaussian kernel (Latore et al. 1998) given by

$$k(x - y) = \frac{1}{2\sqrt{D\pi}} e^{\frac{-(x-y)^2}{4D}}. \quad (3)$$

142 To derive analytical expressions for the critical rates of harvesting and climate velocity, we  
 143 approximate the kernel to its first-order terms, as described in Appendix A.3. Further, to examine  
 144 the sensitivity of the model to the shape of the kernel, we also analyze a sinusoidal kernel (see  
 145 Appendix A.4).

146 At demographic equilibrium, the population will move in a traveling wave, where the population  
 147 density at a given point in space will change, but the density at a location relative to the shifting  
 148 patch will not (Zhou and Kot 2011). The traveling wave  $n^*$  must satisfy

$$n^*(\bar{x}) = \int_{-\frac{L}{2}}^{\frac{L}{2}} k(\bar{x} + c - \bar{y})R_0(1 - h)f(n^*(\bar{y}))d\bar{y}, \quad (4)$$

149 where  $\bar{x}, \bar{y} \in \left[-\frac{L}{2}, \frac{L}{2}\right]$  describes the position within the patch. For a separable kernel, the  
 150 equilibrium traveling pulse  $n^*(x)$  must satisfy

$$n^*(x) = \sum_{i=1}^{\infty} a_i(x) \int_{-\frac{L}{2}}^{\frac{L}{2}} b_i(y - c) R_0(1 - h) f(n^*(y)) dy = \sum_{i=1}^{\infty} m_i a_i(x), \quad (5)$$

151 where the  $m_i$  satisfy the equations

$$m_i = \int_{-\frac{L}{2}}^{\frac{L}{2}} b_i(y - c) R_0(1 - h) f\left(\sum_{j=1}^{\infty} m_j a_j(y)\right) dy \quad (6)$$

152 (Latore et al. 1998). We show the derivation of these equations in Appendix A.2.

### 153 Persistence

154 At low harvesting rates  $h$  and low climate velocities  $c$ , marine populations will persist. However,

155 above certain critical values, populations will be driven extinct. When the population is extinct,

156 the system is in its trivial equilibrium;  $n^*(\bar{x}) = 0$  for all  $x \in \left[-\frac{L}{2}, \frac{L}{2}\right]$ , which satisfies Equation 4.

157 If a population is to persist, it must be able to avoid extinction and grow even when small (Zhou

158 and Kot 2011). Population persistence is therefore equivalent to the trivial traveling pulse being

159 an unstable equilibrium, where the introduction of a small population will grow rather than

160 return to extinction. The critical parameters  $h^*$  and  $c^*$  are defined as the parameters that make the

161 trivial pulse unstable. See Appendix A.1 for further details of this analytical calculation.

162 Regardless of the functional form of the recruitment function  $f$ , the only property that

163 determines whether or not a population can persist is how quickly recruitment increases when the

164 population size is near (but above) 0. For us, this number is 1, and any recruitment function with

165 the same value will give the same results with respect to persistence. Therefore, the population's

166 ability to persist depends on properties of the population itself (the intrinsic growth rate  $R_0$ , the

167 shape of the dispersal kernel, and the expected distance a larva disperses  $\langle d \rangle$ ), properties of the

168 environment (the length of the viable patch  $L$  and how quickly the environment shifts  $c$ ), and the  
169 harvesting rate  $h$ . For a Gaussian kernel, the critical rates  $c^*$  and  $h^*$  are those values of  $c$  and  $h$   
170 such that

$$R_0(1-h)2\sqrt{2}\exp\left(\frac{-c^2}{8D}\right)\left[\operatorname{erf}\left(\frac{L-c}{2\sqrt{2D}}\right)-\operatorname{erf}\left(\frac{-L-c}{2\sqrt{2D}}\right)\right]=1. \quad (7)$$

171  
172 We derive a similar expression for a sinusoidal kernel in the Appendix A.4. We realize that this  
173 formula is not straightforward to understand. For both Gaussian and sinusoidal kernels, however,  
174 we can approximate the critical harvesting proportion by a function that looks like

$$h^* \sim 1 - \frac{1}{R_0} \cdot p(L, R_0)q(\langle d \rangle, c^2, L^2 + 3c^2), \quad (8)$$

175  
176 where  $p$  is a decreasing function of the length of the viable patch and the intrinsic growth rate,  
177 and  $q$  describes how  $h^*$  increases with patch length ( $L$ ) and varies with expected dispersal  
178 distance and climate velocity (see Appendix A.5 for details).

## 179 **Calculating the interaction of climate velocity and harvest**

180 In order to quantify how harvesting interacts with climate velocity, we find the total biomass of  
181 the population when it reaches an equilibrium traveling pulse and compare this equilibrium  
182 biomass in the presence and absence of each stressor individually or the two stressors together.  
183 Equations 5 and 6 allow us to numerically find the total biomass in the equilibrium traveling  
184 pulse under each of these conditions.

185 We use  $B_0$  to denote the equilibrium biomass without either stressor,  $B_h$  the equilibrium biomass  
186 with harvesting but with climate velocity equal to 0,  $B_c$  the equilibrium biomass with climate  
187 velocity greater than 0 but no harvesting, and  $B_{hc}$  the equilibrium biomass with both stressors.  
188 For each stressor or combination of stressors, we calculate the decline in biomass caused by  
189 stressor  $s$  as

$$E_s = B_0 - B_s. \quad (9)$$

190

191 Based upon this definition, there are three kinds of interaction types that can be defined. If the  
192 interaction is purely additive, then the cumulative response to both stressors together would be  
193  $E_{hc} = E_h + E_c$ . If the stressors instead interact synergistically, then  $E_{hc} > E_h + E_c$ . In contrast, the  
194 stressors would interact antagonistically if  $E_{hc} < E_h + E_c$ .

195 We can quantify the degree of synergy as

$$S = E_{hc} - (E_h + E_c). \quad (10)$$

196 where positive  $S$  indicates synergy, negative  $S$  indicates antagonism, and  $S$  of zero indicates  
197 purely additive interactions. This is a common way to measure the interaction among stressors,  
198 though alternative approaches can use the ratio of affected to unaffected biomass as a measure of  
199 effect size (multiplicative model) or consider the effect of the single worst stressor (simple  
200 comparative effects model) (Folt et al. 1999; Crain et al. 2008). The additive model is the most  
201 conservative when quantifying negative effects, as we do here, meaning that it is less likely to  
202 identify synergistic interactions (Folt et al. 2012; Crain et al. 2008).

203

204 **Simulations**

205 We use simulations to implement two management strategies (threshold harvesting rules and  
206 protected areas) that make our basic integrodifference model analytically intractable. Under  
207 threshold harvesting, harvesting pressure is no longer implemented as a proportional removal  
208 from the population. Instead, we evaluate the abundance at each point in space to determine how  
209 much harvesting should occur. If the population abundance is below the designated threshold, no  
210 harvesting occurs. If the population exceeds the threshold, then all the ‘surplus’ individuals are  
211 available to be harvested. This approach is an extreme version of the harvest control rules  
212 proposed for many existing fisheries (Froese et al. 2011).

213 In addition, we introduce networks of protected areas into our simulations by designating  
214 segments of space where the harvesting rate is equal to 0. Protected areas, particularly in the  
215 ocean, are typically designed to meet either harvest management or conservation goals (Agardy  
216 1994; Holland and Brazee 1996; Gaines et al. 2010a), and their spacing and size differ according  
217 to which goal is being pursued. Harvest-oriented protected areas are often designed such that  
218 they maximize adult spillover into harvestable areas by creating many small, closely spaced  
219 reserves (Hastings and Botsford 2003; Gaylord et al. 2005; Gaines et al. 2010a). To mimic this  
220 management scheme, we implemented protected areas with a length 1/3 of the average dispersal  
221 distance and an inter-reserve spacing 2/3 of the average dispersal distance. Conservation-  
222 oriented protected areas seek to protect entire ecosystems and reduce adult spillover by creating  
223 fewer, larger protected areas (Toonen et al. 2013). To mimic this scheme, we implement  
224 protected areas with a length 4 times the average dispersal distance and an inter-reserve spacing  
225 8 times the average dispersal distance between them (Lockwood et al. 2002). In both harvest-  
226 oriented and conservation-oriented protected area networks, 1/3 of the coastline is protected.

227 With protected areas present we assume that harvesting is shifted to available, unprotected  
228 habitat such that harvesting pressure remains constant (see Appendix A.7 for simulations in  
229 which harvest is proportional to areas between reserves).  
  
230 For every simulation, we seed the model with 50 individuals at a single location and iterate for  
231 2000 generations to reach equilibrium without harvesting or climate shift (more than sufficient  
232 based on initial tests). We then add harvesting pressure, allow the population to again reach  
233 equilibrium (2000 generations), and finally add a changing climate by moving the viable patch  
234 with a certain velocity. After 6000 generations we calculate equilibrium biomass as the mean  
235 biomass of 2000 additional generations. Implementing protected areas makes the population  
236 abundance cycle, but averaging over 2000 generations is sufficient to erase the effects of  
237 periodicity in our results. If population abundance declines below 0.001, the population is  
238 considered extinct (i.e. abundance is 0). For all simulations, we use a Laplace dispersal kernel,  
239  $k(x - y) = \frac{1}{2}be^{-b|x-y|}$ , which is a commonly used model of marine larval dispersal (Botsford  
240 et al. 2001) and which is not amenable to the analytical methods we use above.

## 241 **Results**

### 242 **Persistence with Harvesting and Climate Velocity**

243 We begin by examining the critical rates of harvesting and climate velocity, i.e., those rates  
244 sufficient to drive a population extinct. As would be expected, we find that the critical rate of  
245 each stressor is lower if a population faces higher intensities of the other stressor (downward  
246 curving lines in Figure 1). For example, a harvesting rate that is sustainable in the absence of

247 environmental shift ( $c$  near zero) may no longer be sustainable if the environment begins to  
248 change rapidly ( $c \gg$  zero).

249 We also examine the sensitivity of critical rates to growth and dispersal. In our model, it is  
250 always the case that increasing the intrinsic growth rate ( $R_0$ ), all else being equal, will increase  
251 the critical climate velocity  $c^*$  and the critical harvesting rate  $h^*$ , since a population that grows  
252 more quickly can recover more effectively from losses caused by these stressors (compare lines  
253 with different shading in Figure 1). However, whether or not dispersing farther is better depends  
254 on how quickly the environment is shifting (compare solid and dashed lines in Figure 1). When  
255 the environment is shifting slowly, populations with wider dispersal kernels have a lower critical  
256 harvesting rate because dispersing farther results in too many larvae dispersing off the viable  
257 patch. When the environment is shifting quickly, on the other hand, populations with wider  
258 dispersal kernels can better withstand harvesting because larvae dispersing long distances more  
259 effectively colonize the habitat patch that will be viable in the next generation.

## 260 **Interactions Between Stressors**

261 It is also important to ask how a population responds to moderate cumulative impacts that are  
262 insufficient to drive it extinct. Whenever climate velocity or harvesting pressure exceeds their  
263 critical rate, the biomass of the population at equilibrium will be equal to 0 (the definition of the  
264 critical rate). Before the stressors reach those thresholds, however, the equilibrium biomass of  
265 the population decreases smoothly as either the harvesting pressure or the rate of environmental  
266 shift increases (Figure 2a).

267 When we compare the cumulative impacts of the stressors to the sum of each stressor  
268 individually we find low levels of positive synergy between the two stressors (Figure 2b). The

269 stressors display a synergistic interaction most strongly at high harvest and climate velocity rates,  
270 close to where they would drive the population extinct. As a note, positive synergy indicates that  
271 cumulative impacts cause the population to lose more biomass than we would predict from either  
272 stressor individually. However, the degree of synergy is low and concentrated in a limited part of  
273 parameter space. Throughout much of the range of harvest rates and climate velocities, the  
274 interaction between the stressors is quite close to an additive model. Results are robust to  
275 changes from a Gaussian to a sinusoidal dispersal kernel.

## 276 **Alternative management strategies**

277 Under a constant harvest rate, we find that harvest rate and climate velocity interact such that  
278 more heavily harvested populations go extinct with slower climate velocities. However, with  
279 harvest thresholds in place, a small population can always escape harvesting and the critical  
280 climate velocity  $c^*$  no longer depends on the harvesting rate (Figure 3b). In other words, as long  
281 as there is some threshold population density below which harvesting is not allowed, critical  
282 climate velocity in our model only depends on the growth rate, length of the viable patch, and  
283 average dispersal distance. In this case, the interaction follows a simple comparative model, such  
284 that the cumulative impacts of the two stressors are equal to the individual effect of the worst  
285 stressor.

286 With protected areas present we either assume that harvesting is proportional in areas between  
287 reserves or that harvesting pressure remains constant, and is shifted to available, unprotected  
288 habitat. We find our results are qualitatively identical: effort reallocation effectively increases the  
289 harvest rate, reducing the critical harvest rate. We present the following results for MPAs  
290 without effort reallocation (see Appendix A.7 for details, Figure S2). With either type of  
291 protected area strategy in effect (many small versus few large), the population withstands

292 combinations of higher climate velocities and higher harvesting rates than without the protected  
293 areas (compare Figures 3c and d to Figure 3a). However, there are also differences between the  
294 large and the small protected area strategies. At lower climate velocities, protected areas spaced  
295 more than one average dispersal distance apart result in larger fluctuations of population biomass  
296 relative to small, closely spaced protected areas (Appendix A.6, Figure S1). Minimum  
297 population biomass is higher in simulations with smaller protected areas, potentially providing a  
298 larger buffer against extinction relative to simulations with larger but more widely spaced  
299 protected areas.

## 300 **Discussion**

301 Climate change and harvest are two of the dominant human impacts on marine species and many  
302 terrestrial species, but our understanding for their joint effects and interactions remains limited.  
303 By analyzing a general model that incorporates dispersal and reproduction, we show that climate  
304 velocity and harvesting interact strongly in their effects on species persistence and biomass. In  
305 particular, we find that the critical harvesting rate decreases as climate velocity increases. In  
306 other words, the more quickly the environment shifts, the less harvesting it takes to drive the  
307 population extinct. The interaction between climate velocity and harvesting are additive for most  
308 combinations of stressor levels, with weak synergy only appearing close to population extinction.  
309 However, harvesting rules that avoid harvest from low-density parts of the population, such as  
310 the leading edge, change the interaction substantially. In the latter case, the population only  
311 decreases by an amount equal to the effect of the single worst stressor (whether climate velocity  
312 or harvest).

313 Our results suggest that particular combinations of harvesting and climate velocity will affect  
314 certain species more than others. Species with a higher intrinsic population growth rate (i.e.,  
315 growth rate at low abundance) and a longer average dispersal distance will better track rapid  
316 climate velocities, as compared to species with a low intrinsic population growth rate and short  
317 dispersal distances. This finding matches previous expectations: higher growth rates make a  
318 population more resistant to the removals from harvesting or the losses associated with tracking  
319 climate velocity. It is worth pointing out that a higher population growth rates can be generated  
320 either by shorter generation times or higher fecundity. Empirical work also suggests that marine  
321 fish and invertebrates with faster life histories, as well as terrestrial birds and plants with greater  
322 dispersal abilities, shifted their distributions more quickly in response to warming (Perry et al.  
323 2005; Angert et al. 2011; Pinsky et al. 2013).

324 While higher reproductive rates improve a population's ability to persist in our model, higher  
325 dispersal distances did not necessarily do so. In agreement with related results from Zhou and  
326 Kot (2011), we found that at low speeds, a short dispersal distance improved the maximum  
327 harvesting rate a population could sustain, while at higher speeds a longer dispersal distance  
328 improved the maximum climate velocity under which the population could persist. It appears that  
329 climate velocity could selectively favor species with dispersal distances best matched to the rate  
330 of shift.

331 One goal of our model is to examine the cumulative impacts of multiple stressors. We find that  
332 the interaction between harvest and climate velocity is effectively additive, with weak synergistic  
333 effects appearing primarily when the population is close to extinction. This result from our  
334 model would appear to contrast with other demonstrations of synergy between harvest and  
335 climate in the literature. For example, a number of modeling and empirical studies have found

336 that fishing increases the sensitivity of populations to climate variability (including Anderson et  
337 al. 2008; Shelton et al. 2011; Botsford et al. 2011), and a recent review reaches the same  
338 conclusion (Planque et al. 2010). Positive feedback loops involving the loss of predators due to  
339 fishing have also been identified that amplify climate impacts on prey species (Kirby et al. 2009;  
340 Planque et al. 2010; Ling et al. 2009). Similarly, synergy between harvesting and temperature  
341 was detected in experimental populations of rotifers (Mora et al. 2007).

342 A partial explanation for the differences between our model results and the previous evidence for  
343 synergy may be that we analyze the ability of populations to keep pace with climate velocity,  
344 while many previous studies examined other aspects of changing climate. In the rotifer  
345 experiment, for example, populations were subjected to warming temperatures, but organisms  
346 were unable to relocate to thermal optima (Mora et al. 2007). In many other fishing and climate  
347 studies, the impacts of climate variability on stationary populations have been the focus, rather  
348 than cumulative climate change or shifting distributions (Walters and Parma 1996; Anderson et  
349 al. 2008; Shelton et al. 2011; Botsford et al. 2011; Planque et al. 2010). Work that does  
350 incorporate shifting species distributions typically examines regional or global scenarios for  
351 climate change, making it difficult to isolate the effect that different species interactions, climate  
352 and harvesting each play (Cheung et al. 2010).

353 Another explanation for the discrepancy may be that the only effect of harvesting in our model is  
354 a reduction in the size of the adult biomass. In reality, populations often contain a diversity of  
355 subpopulations, ages, and genotypes that can buffer them against climate variability and climate  
356 change (Schindler et al. 2010). Harvest tends to simplify this diversity within populations,  
357 making them more sensitive to climate variability (Mora et al. 2007; Planque et al. 2010). Our  
358 model also did not include food web dynamics or species interactions, although some positive

359 feedback loops and synergistic interactions identified between climate and harvesting in previous  
360 studies involved the loss of predators and the release of prey (Kirby et al. 2009; Ling et al. 2009).  
361 Our simple, single-species, non-age-structured model suggests that additive interactions between  
362 climate velocity and harvesting constitute a reasonable baseline or “null” expectation in the  
363 absence of more complicated mechanisms. Future work considering food web processes and  
364 genetic, spatial, and age diversity will be important to examine other possible sources of  
365 synergistic (or antagonistic) interactions between harvesting and climate velocity.

366 We also examine whether two frequently recommended management approaches, protected  
367 areas and harvest control rules, could help ensure species persistence in the face of multiple  
368 stressors. With either of these management strategies, we generally find increases in the  
369 population’s biomass at equilibrium and an improved ability to persist. Threshold harvesting  
370 rules in particular appear to fundamentally alter much of the interaction between the two  
371 stressors. In our model, thresholds appear to have this effect because they effectively prevent  
372 harvesting of the leading edge and allow colonization to occur as if these individuals were  
373 moving into un-harvested areas. This result matches well with invasion theory, which has shown  
374 that populations move into new territory at a rate approximately equal to  $2\sqrt{R_0 l}$ , where  $l$  is the  
375 mean squared displacement of individuals per unit time (Fisher 1937). With a constant harvest  
376 rate applied everywhere, the invasion rate drops to  $2\sqrt{(1 - h)R_0 l}$ , whereas the invasion rate is  
377 unaffected if harvesting avoids the leading edge. It’s interesting to note that novel, low  
378 abundance stocks are commonly unregulated in fisheries systems (Beddington et al. 2007;  
379 Dowling et al. 2008). Whether fisheries and other harvesting activities rapidly exploit newly  
380 colonizing species depends in part on the interaction of social, economic, and regulatory factors  
381 (Pinsky and Fogarty 2012). Our work, however, highlights the fact that a low (or zero) harvest

382 rate on species that have recently colonized new habitats can be important for helping them keep  
383 up with rapid climate velocities.

384 Unlike thresholds, protected areas are spatially explicit. Previous work has advanced protected  
385 areas as a way to help organisms keep pace with shifting climates, as well as to ameliorate  
386 anthropogenic disturbances like harvesting and habitat fragmentation (Lawler et al. 2010;  
387 Hannah et al. 2007; Botsford et al. 2001; Gaylord et al. 2005; Hastings and Botsford 2003;  
388 Thomas et al. 2012, Watson et al. 2011). Our results show that protected areas increase the  
389 equilibrium biomass of harvested populations at a given climate velocity, which supports their  
390 use as a tool to help these populations withstand the effects of climate velocity. However, the  
391 details of protected-area design affect our results: few, large protected areas increase population  
392 fluctuations at low climate velocities, while many smaller protected areas maintain a population  
393 bounded farther from extinction. This effect appears because large gaps separate our large  
394 protected areas, which allows harvest to drive populations to lower levels while between  
395 protected areas. In contrast, populations were less exposed to harvesting while traversing the  
396 smaller gaps between small protected areas. While the discussion of many small vs. few large  
397 protected areas involves many factors (Gaines et al. 2010b; McCarthy et al. 2011), our results  
398 contribute to this body of work by showing that small gaps between protected areas, even if  
399 counter-balanced by small protected areas, may help species keep up with climate velocities in  
400 the face of harvest.

401 The advantage of a simple model like ours is that it is potentially general enough to apply to a  
402 wide range of species. Our discrete-time, continuous-space model captures the processes  
403 important to species with distinct growth and dispersal stages, including most marine organisms,  
404 plants, trees, and many insects. Our approach does not capture all the complexities of real

405 populations or of harvesting dynamics, however. For example, we do not include the potential  
406 for negative per capita growth at low densities, often called Allee or depensation effects.  
407 Invasion theory suggests that Allee effects generally have two impacts: they slow initial rates of  
408 spread, and they allow predation to, in some cases, slow or stop an invasion (Hastings et al.  
409 2005). Based on first principles, we would expect similar effects in a model like ours, suggesting  
410 that populations with Allee effects will be more sensitive to the combined effects of harvest and  
411 climate velocity than our model initially suggests. We also did not include age structure or other  
412 aspects of sub-population diversity (e.g., spatial or genetic) in our model. As described above,  
413 these forms of diversity have been important for studying the joint effects of harvesting and  
414 climate variability (Botsford et al. 2011; Planque et al. 2010), and will likely be important for  
415 understanding climate velocity impacts as well. Besides these species-specific extensions, this  
416 modeling framework could also be extended to consider species interactions, such as between  
417 predator and prey (Gilman et al. 2010). A final important extension is better capturing harvesting  
418 dynamics. We find that the distribution of harvesting pressure affects the outcomes of our simple  
419 model (i.e. thresholds, versus proportional harvesting). Harvester behavior, to the extent it has  
420 been considered in fisheries, highlights considerable uncertainty in how vessels allocate effort  
421 over space and respond to changes in environmental conditions (Fulton et al. 2011, Van Putten et  
422 al. 2011, Pinsky and Fogarty 2012). These responses are rarely integrated into modeling efforts,  
423 and an important next step is integrated assessments of social-ecological systems.

424 Using a simple, mechanistic model like the one we present here helps to build intuition about the  
425 conditions under which species can survive the cumulative impacts of climate and harvesting.  
426 This work highlights the importance of considering stressors in combination, as outcomes  
427 deviate from what we would predict in isolation. It also shows the importance of alternative

428 management strategies, as the location of harvest greatly affects the interaction between  
429 harvesting and climate. While management strategies only change harvesting practices and do  
430 not directly address climate change, understanding how management approaches can affect  
431 interactions between harvesting and range shifts will help to improve harvesting rules and the  
432 development of protected areas. Our results are encouraging evidence that management practices  
433 can help protect marine populations from the cumulative impacts of harvesting and climate  
434 change.

## 435 Acknowledgements

436 We thank Catherine Offord and Will Scott for discussions on this project, and James Watson,  
437 Emily Klein and Simon Levin for comments on an earlier draft. EF acknowledges support from  
438 the National Science Foundation (GRFP, GEO-1211972), EB acknowledges support from the  
439 National Institute of Health (NIH 5T32HG003284), and MP acknowledges support from a David  
440 H. Smith Conservation Research Fellowship.

## 441 Literature Cited

- 442 Agardy, M. Tundi. 1994. Advances in marine conservation: the role of marine protected areas.  
443 *Trends in Ecology & Evolution* 9: 267–270.
- 444 Anderson, C.N.K., et al. 2008. Why fishing magnifies fluctuations in fish abundance. *Nature*  
445 452: 835–9.
- 446 Angert, A.L., L. G. Crozier, L. J. Rissler, S. E. Gilman, J. J. Tewksbury and A. J. Chunco, 2011.  
447 Do species' traits predict recent shifts at expanding range edges? *Ecology Letters* 14: 677–89.
- 448 Beddington, J.R., D. J. Agnew, and C. W. Clark. 2007. Current problems in the management of  
449 marine fisheries. *Science* 316: 1713–6.
- 450 Berestycki, H., O. Diekmann, C. J. Nagelkerke, and P. A. Zegeling. 2009. Can a species keep  
451 pace with a shifting climate? *Bulletin of Mathematical Biology* 71: 399–429.

- 452 Botsford, L. W., A. Hastings, and S. D. Gaines. 2001. Dependence of sustainability on the  
453 configuration of marine reserves and larval dispersal distance. *Ecology Letters* 4: 144–150.
- 454 Botsford, L. W., M. D. Holland, J. F. Samhouri, J. W. White, and A. Hastings. 2011. Importance  
455 of age structure in models of the response of upper trophic levels to fishing and climate change.  
456 *ICES Journal of Marine Science: Journal du Conseil* 68: 1270–1283.
- 457 Burrows, M. T., et al. 2011. The pace of shifting climate in marine and terrestrial ecosystems.  
458 *Science* 334: 652-5.
- 459 Byers, J. E. and J. M. Pringle. 2006. Going against the flow: retention, range limits and invasions  
460 in advective environments. *Marine Ecology Progress Series* 313: 27-41.
- 461 Chen, I. C., J. K. Hill, R. Ohlemüller, D. B. Roy, and C. D. Thomas. 2011. Rapid range shifts of  
462 species associated with high levels of climate warming. *Science* 333: 1024-6.
- 463 Cheung, W. W. L., V. W. Y. Lam, J. L. Sarmiento, K. Kearney, R. E. G. Watson, D. Zeller, and  
464 D. Pauly. 2010. Large-scale redistribution of maximum fisheries catch potential in the global  
465 ocean under climate change. *Global Change Biology* 16: 24–35.
- 466 Crain, C. M., K. Kroeker, and B. S. Halpern. 2008. Interactive and cumulative effects of multiple  
467 human stressors in marine systems. *Ecology Letters* 11: 1304–15.
- 468 Darling, E. S., and I. M. Côté. 2008. Quantifying the evidence for ecological synergies. *Ecology  
Letters* 11: 1278–86.
- 470 Doak, D. F., and W. F. Morris. 2010. Demographic compensation and tipping points in climate-  
471 induced range shifts. *Nature* 467: 959–62.
- 472 Dowling, N. A., et al. 2008. Developing harvest strategies for low-value and data-poor fisheries:  
473 Case studies from three Australian fisheries. *Fisheries Research* 94: 380–390.
- 474 Elith, J., et al. 2006. methods improve prediction of species' distributions from occurrence data.  
475 *Ecography* 29: 129–151.
- 476 Engelhard, G.H., D. A. Righton, and J. K. Pinnegar. 2014. Climate change and fishing: a century  
477 of shifting distribution in North Sea cod. *Global Change Biology*. doi: 10.1111/gcb.12513
- 478 Fisher, R.A. 1937. The wave of advance of advantageous genes. *Annals of Eugenics* 7: 355-369.
- 479 Folt, C. L., C. Y. Chen, M. V. Moore, and J. Burnaford. 1999. Synergism and antagonism among  
480 multiple stressors. *Limnology and Oceanography* 44: 864–877.
- 481 Fordham, D. A. A., et al. 2013. Population dynamics can be more important than physiological  
482 limits for determining range shifts under climate change. *Global Change Biology* 19: 3224-3237.
- 483 Froese, R., T. A. Branch, A. Proelß, M. Quaas, K. Sainsbury, and C. Zimmermann. 2011.  
484 Generic harvest control rules for European fisheries. *Fish and Fisheries* 12: 340–351.
- 485
- 486 Fulton, E. A., A. D. M. Smith, D. C. Smith, D. C., and I. E. van Putten. 2011. Human behaviour:  
487 The key source of uncertainty in fisheries management. *Fish and Fisheries*, 12: 2-17.

- 488 Gaines, S. D., C. White, M. H. Carr, and S. R. Palumbi. 2010a. Designing marine reserve  
489 networks for both conservation and fisheries management. *Proceedings of the National Academy*  
490 *of Sciences USA* 107: 18286–93.
- 491 Gaines, S. D., S. E. Lester, K. Grorud-Colvert, C. Costello, and R. Pollnac. 2010b. Evolving  
492 science of marine reserves: new developments and emerging research frontiers. *Proceedings of*  
493 *the National Academy of Sciences USA* 107: 18251–5.
- 494 Gaylord, B., S. D. Gaines, D. A. Siegel, and M. H. Carr. 2005. Marine reserves exploit  
495 population structure and life history in potentially improving fisheries yields. *Ecological*  
496 *Applications* 15: 2180–2191.
- 497 Gilman, S.E., M. C. Urban, J. J. Tewksbury, G. W. Gilchrist, and R. D. Holt. 2010. A framework  
498 for community interactions under climate change. *Trends in Ecology and Evolution* 25: 325–331.
- 499 Guisan, A. and W. Thuiller. 2005. Predicting species distribution: offering more than simple  
500 habitat models. *Ecology Letters* 8: 993–1009.
- 501 Guisan, A. and N. E. Zimmermann. 2000. Predictive habitat distribution models in ecology.  
502 *Ecological modelling* 135: 147–186.
- 503 Gurevitch, J., J. A. Morrison, and L. V. Hedges. 2000. The Interaction between Competition and  
504 Predation: A Metaanalysis of Field Experiments. *The American Naturalist* 155: 435–453.
- 505 Halpern, B. S., et al. 2008. A global map of human impact on marine ecosystems. *Science* 319:  
506 948–52.
- 507 Hannah, L., G. Midgley, S. Andelman, M. Araújo, G. Hughes, E. Martinez-Meyer, R. Pearson,  
508 and P. Williams. 2007. Protected area needs in a changing climate. *Frontiers in Ecology and the*  
509 *Environment* 5: 131–138.
- 510 Hare, J.A., M. A. Alexander, M. J. Fogarty, E. H. Williams, and J. D. Scott. 2010. Forecasting  
511 the dynamics of a coastal fishery species using a coupled climate-population model. *Ecological*  
512 *Applications* 20: 452–64.
- 513 Hastings, A., et al. 2005. The spatial spread of invasions: new developments in theory and  
514 evidence. *Ecology Letters* 8: 91–101.
- 515 Hastings, A. and L. W. Botsford. 2003. Comparing designs of marine reserves for fisheries and  
516 for biodiversity. *Ecological Applications* 13: 65–70.
- 517 Holland, D. S., and R. J. Brazee. 1996. Marine reserves for fisheries management. *Marine*  
518 *Resource Economics* 11: 157–172.
- 519 Kearney, M. and W. Porter. 2009. Mechanistic niche modelling: combining physiological and  
520 spatial data to predict species' ranges. *Ecology Letters* 12: 334–50.
- 521 Kirby, R. R., G. Beaugrand, and J. A. Lindley. 2009. Synergistic Effects of Climate and Fishing  
522 in a Marine Ecosystem. *Ecosystems* 12: 548–556.

- 523 Kot, M. and W. M. Schaffer. 1986. Discrete-time growth-dispersal models. Mathematical  
524 Biosciences 80: 109–136.
- 525 Latore, J., P. Gould, and A. M. Mortimer. 1998. Spatial dynamics and critical patch size of  
526 annual plant populations. *Journal of Theoretical Biology* 190: 277–285.
- 527 Lawler, J. J., et al. 2010. Resource management in a changing and uncertain climate. *Frontiers in  
528 Ecology and the Environment* 8: 35–43.
- 529 Ling, S. D., C. R. Johnson, S. D. Frusher, and K. R. Ridgway. 2009. Overfishing reduces  
530 resilience of kelp beds to climate-driven catastrophic phase shift. *Proceedings of the National  
531 Academy of Sciences USA* 106: 22341–22345.
- 532 Loarie, S. R. P. B. Duffy, H. Hamilton, G. P. Asner, C. B. Field, and D. D. Ackerly. 2009. The  
533 velocity of climate change. *Nature*, 462: 1052–5.
- 534 Lockwood, D. R., A. Hastings, and L. W. Botsford. 2002. The effects of dispersal patterns on  
535 marine reserves: does the tail wag the dog? *Theoretical Population Biology* 61: 297–309.
- 536 McCarthy, M.A., C. J. Thompson, A. L. Moore, and H. P. Possingham. 2011. Designing nature  
537 reserves in the face of uncertainty. *Ecology Letters* 14: 470–5.
- 538 Milner-Gulland, J., and E. L. Bennett. 2003. Wild meat: The bigger picture. *Trends in Ecology &  
539 Evolution*, 18: 351–357.
- 540 Mora, C., R. Metzger, A. Rollo, and R. A. Myers. 2007. Experimental simulations about the  
541 effects of overexploitation and habitat fragmentation on populations facing environmental  
542 warming. *Proceedings of the Royal Society B* 274: 1023–1028.
- 543 Nye, J. A., R. J. Gamble, and J. S. Link. 2013. The relative impact of warming and removing top  
544 predators on the Northeast US large marine biotic community. *Ecological Modelling* 264: 157–  
545 168.
- 546 Pelletier, E., P. Sargian, J. Payet, and S. Demers. 2006. Ecotoxicological effects of combined  
547 UVB and organic contaminants in coastal waters: a review. *Photochemistry and photobiology*  
548 82: 981–993.
- 549 Perry, A. L., P. J. Low, J. R. Ellis, and J. D. Reynolds. 2005. Climate Change and Distribution  
550 Shifts in Marine Fishes. *Science* 308: 1912–1915.
- 551 Pimm, S., et al. 2001. Can we defy nature's end? *Science*, 293: 2207–2208.
- 552 Pinsky, M. 2011. Dispersal, Fishing, and the Conservation of Marine Species. Stanford  
553 University: Stanford University.
- 554 Pinsky, M. L., and M. Fogarty. 2012. Lagged social-ecological responses to climate and range  
555 shifts in fisheries. *Climatic Change* 115: 883–891.
- 556 Pinsky, M. L., B. Worm, M. J. Fogarty, J. L. Sarmiento, and S. A. Levin. 2013. Marine taxa  
557 track local climate velocities. *Science* 341: 1239–42.

- 558 Planque, B., J. Fromentin, P. Cury, K. F. Drinkwater, S. Jennings, R. I. Perry, and S. Kifani.  
559 2010. How does fishing alter marine populations and ecosystems sensitivity to climate? *Journal*  
560 *of Marine Systems* 79: 403–417.
- 561 Robinson, L. M. M., J. Elith, A. J. J. Hobday, R. G. G. Pearson, B. E. E. Kendall, H. P. P.  
562 Possingham, and A. J. J. Richardson. 2011. Pushing the limits in marine species distribution  
563 modelling: lessons from the land present challenges and opportunities. *Global Ecology and*  
564 *Biogeography* 20: 789–802.
- 565 Schindler, D.E., et al. 2010. Population diversity and the portfolio effect in an exploited species.  
566 *Nature* 465: 609–12.
- 567 Sala, O. E. E., et al. 2000. Global biodiversity scenarios for the year 2100. *Science* 287: 1770–  
568 1774.
- 569 Sekercioglu, C. H., S. H. Schneider, J. P. Fay, and S. R. Loarie. 2008. Climate Change,  
570 Elevational Range Shifts, and Bird Extinctions. *Conservation Biology* 22: 140-150.
- 571 Shelton, A.O. and M. Mangel. 2011. Fluctuations of fish populations and the magnifying effects  
572 of fishing. *Proceedings National Academy Sciences USA* 108: 7075–7080.
- 573 Thomas, C. D., et al. 2012. Protected areas facilitate species' range expansions. *Proceedings of*  
574 *the National Academy of Sciences USA* 109: 14063–8.
- 575 Toonen, R.J., et al. (2013). One size does not fit all: the emerging frontier in large-scale marine  
576 conservation. *Marine Pollution Bulletin* 77: 7–10.
- 577 Travis, J. M. J.. 2003. Climate change and habitat destruction: a deadly anthropogenic cocktail.  
578 *Proceedings of the Royal Society B: Biological Sciences* 270 (1514): 467-73.
- 580 Van Kirk, R. W. and M. A. Lewis. 1997. Integrodifference models for persistence in fragmented  
581 habitats. *Bulletin of Mathematical Biology* 59: 107–137.
- 582 van Putten, I. E., S. Kulmala, O. Thébaud, N. Dowling, K. G. Hamon, T. Hutton, and S. Pascoe.  
583 2011. Theories and behavioural drivers underlying fleet dynamics models. *Fish and Fisheries*  
584 13: 216-235.
- 585 Walters, C., and A. M. Parma. 1996. Fixed exploitation rate strategies for coping with effects of  
586 climate change. *Canadian Journal of Fisheries and Aquatic Sciences* 53: 148–158.
- 587 Watson, J. R., D. A. Siegel, B. E. Kendall, S. Mitarai, A. Rassweiller, and S. D. Gaines. 2011.  
588 Identifying critical regions in small-world marine metapopulations. *Proceedings of the National*  
589 *Academy of Sciences USA* 108: e907-e913.
- 590 Wilcove, D. S., D. R., J. Dubow, A. Phillips, and E. Losos. 1998. Quantifying threats to  
591 imperiled species in the United States. *BioScience* 48: 607–615.
- 592 Worm, B., et al. 2009. Rebuilding global fisheries. *Science* 325: 578-585.

- 593 Zarnetske, P. L., D. K. Skelly, and M. C. Urban. 2012. Ecology. Biotic multipliers of climate  
594 change. *Science* 336: 1516–8.
- 595 Zhou, Y., and M. Kot. 2011. Discrete-time growth-dispersal models with shifting species ranges.  
596 *Theoretical Ecology* 4: 13–25.

597

598 **Tables**

599 **Table 1: Parameter values and functions used in the text**

| Variable            | Definition   |
|---------------------|--|
| $n_t(x)$            | density of individuals at position $x$ at time $t$   |
| $n^*(\bar{x})$      | density of individuals at equilibrium at position $\bar{x}$ relative to the patch                  |
| $k(x - y)$          | dispersal kernel, the probability of offspring traveling from position $y$ to position $x$         |
| $\langle d \rangle$ | expected distance traveled by an offspring   |
| $f(n)$              | recruitment function, the number of offspring produced by a population of size $n$                 |
| $R_0$               | intrinsic growth rate of the population at low abundance   |
| $g(n)$              | harvest function, the number of adults remaining after a population of size $n$ has been harvested |
| $h$                 | proportion of adults harvested, when $g(n) = hn$   |
| $L$                 | patch length   |
| $c$                 | climate velocity in units of distance per time   |

600

601 **Figure Legends**  
602

603 Figure 1: (a) Lines indicate the critical threshold for persistence as a function of harvesting rate  
604 on the y-axis and climate velocity on the x-axis. Shade of grey corresponds to the growth rate  
605 from smallest to greatest (light to dark). Line style indicates the average dispersal distance (solid:  
606  $\langle d \rangle = 0.1$  vs. dashed:  $\langle d \rangle = 0.5$ ) from an approximated Gaussian dispersal kernel (Eq. 3). Patch  
607 length  $L = 1$ .

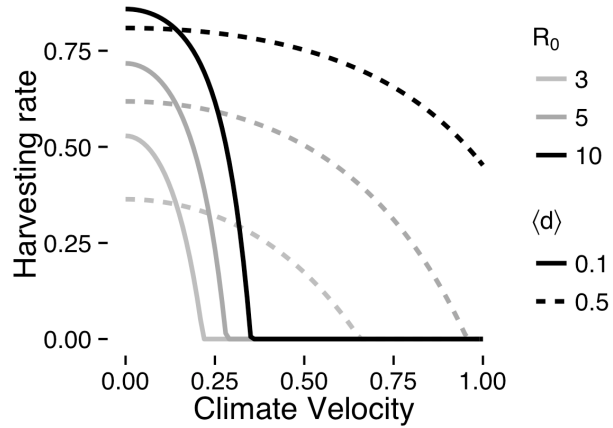
608 Figure 2: (a) The equilibrium biomass of the population as a function of the climate velocity on  
609 the x-axis and the proportional harvesting rate on the y-axis. Results are from an approximated  
610 Gaussian dispersal kernel with parameters  $L = 1$ ,  $R_0 = 10$ , and  $\langle d \rangle = 0.5$ . (b) Interaction  
611 between the two stressors as a function of climate velocity and harvesting rate. Shading indicates  
612 the degree of synergistic interaction, i.e., the loss in biomass in the doubly stressed population in  
613 excess of the sum of the losses caused by each stressor individually ( $E_{hc} - E_h - E_c$ ). Synergy of  
614 0 indicates additive interaction of the stressors. The excess loss, on the order of 0.001, is small in  
615 comparison to the total biomass, which can be as large as 20. These results are from calculations  
616 with the same parameters as Figure 2a.

617 Figure 3: The equilibrium biomass of the population as a function of the climate velocity on the  
618 x-axis and the harvesting rate on the y-axis under alternative management strategies. (a) The  
619 equilibrium biomass for simulations with constant harvest rates (compare to figure 2a). (b)  
620 Equilibrium biomass for simulations with threshold management. For threshold management, the  
621 maximum threshold is set to be the largest population size observed at a given time step before  
622 harvesting. The y-axis is the proportion of the maximum threshold that is protected from  
623 harvesting. (c) Equilibrium biomass for simulations with many small protected areas. (d)  
624 Equilibrium biomass for simulations with few large protected areas. These results are from a  
625 simulation with a Laplacian dispersal kernel with parameters  $L = 1$ ,  $R_0 = 5$ ,  $K = 100$ , and  
626  $\langle d \rangle = 2$ .

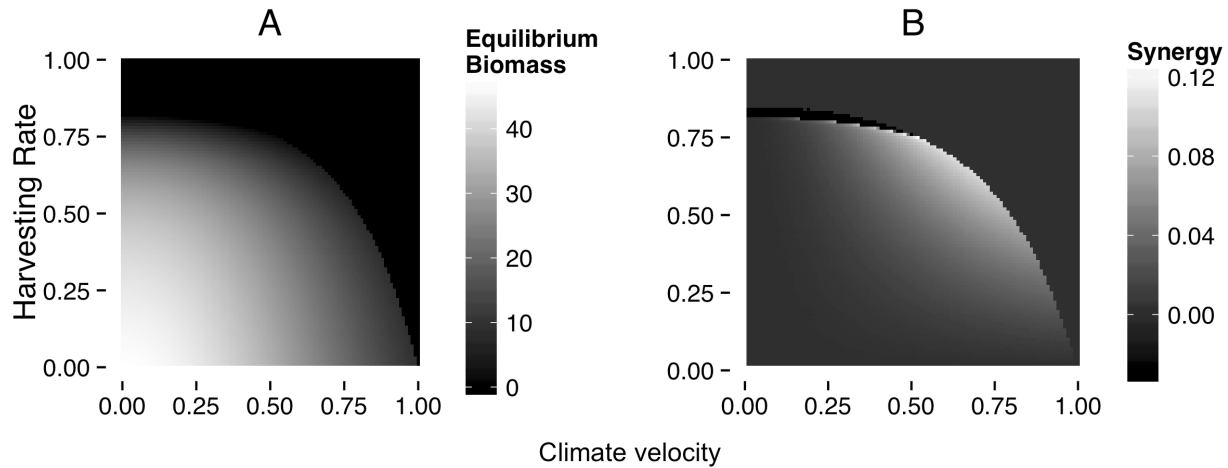
627

628 **Figures**

629

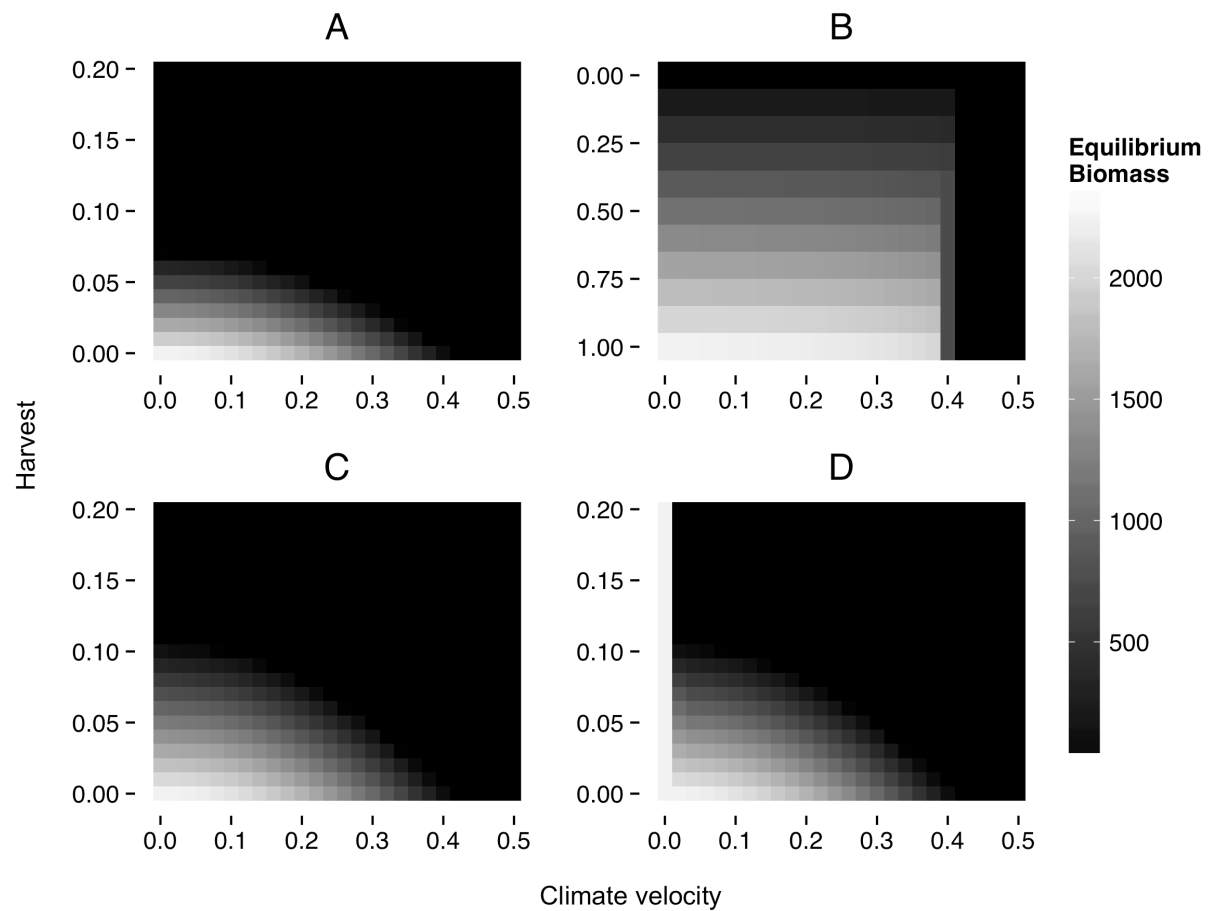


630 Figure 1



631

632 Figure 2



633

634 Figure 3

## A Appendix

In Appendix A.1, we provide the details for assessing the persistence of a population with an integrodifference model and we discuss the effect of the harvesting function on population persistence. In Appendix A.2, we provide the details for assessing population persistence with separable dispersal kernels. In Appendix A.3 and A.4, we derive expressions for the critical harvesting rate and rate of environmental shift for Gaussian and sinusoidal dispersal kernels. In Appendix A.5, we derive approximate expressions for these critical rates. In Appendix A.6 we provide details on differences between small and large MPA simulations. In Appendix A.7 we show how reallocation of effort does not qualitatively change our results in our MPA simulations.

**A.1 Determining stability** Let  $n_t(x)$  be the number of adults at position  $x$  at time  $t$ , let  $k(x)$  be a dispersal kernel describing the probability of a larva traveling a distance  $x$ , let  $f(n)$  be the recruitment function describing the number of offspring that settle and survive in juvenile population of size  $n$ , let  $R_0$  be the intrinsic growth rate of the population, and let  $g(n)$  be the harvesting function describing the number of adults harvested from a population of size  $n$ . In the absence of harvesting, the integrodifference model describing the population over time is given by

$$n_{t+1}(x) = \int_{-L/2+ct}^{L/2+ct} k(x-y) R_0 f(n_t(y)) dy \quad (1)$$

as described in Zhou and Kot [2011]. With the addition of harvesting, the model becomes

$$n_{t+1}(x) = \int_{-L/2+ct}^{L/2+ct} k(x-y) R_0 g(f(n_t(y))) dy. \quad (2)$$

In evaluating persistence, we apply the methods of Zhou and Kot [2011] to the new model, Equation 2. A traveling pulse is a solution such that population size relative to location within the patch (rather than absolute position) is constant over time, i.e.

$$n^*(\bar{x}_t) \equiv n^*(x - ct) = n_t(x),$$

where  $\bar{x}_t \equiv x - ct$  gives position relative to the patch.

The integrodifference equation (2) gives us an expression for  $n^*$ :

$$\begin{aligned}
n^*(\bar{x}_{t+1}) &= n_{t+1}(x) \\
&= \int_{-L/2+ct}^{L/2+ct} k(x-y) R_0 g(f(n_t(y))) dy \\
&= \int_{-L/2+ct}^{L/2+ct} k(x - \bar{y}_t - ct) R_0 g(f(n^*(\bar{y}_t))) dy \\
&= \int_{-L/2+ct}^{L/2+ct} k(\bar{x}_t - \bar{y}_t) R_0 g(f(n^*(\bar{y}_t))) dy \\
\Rightarrow n^*(\bar{x}_t - c) &= \int_{-L/2+ct}^{L/2+ct} k(\bar{x}_t - \bar{y}_t) R_0 g(f(n^*(\bar{y}_t))) dy \\
\Rightarrow n^*(\bar{x}_t) &= \int_{-L/2}^{L/2} k(\bar{x}_t + c - \bar{y}_t) R_0 g(f(n^*(\bar{y}_t))) d\bar{y}_t
\end{aligned} \tag{3}$$

As long as  $f(0) = 0$ , there is a trivial solution to this problem where  $n^*(\bar{x}) \equiv 0$  for all  $\bar{x}$ , i.e., there is a trivial traveling pulse with no adults in it. If the trivial traveling pulse is unstable, even very small populations will persist or grow and avoid crashing back to the trivial pulse. To evaluate the stability of a traveling pulse, we introduce a small perturbation to the traveling pulse  $n^*(\bar{x})$  and see if this perturbation grows or shrinks over time:

$$\begin{aligned}
n_t(x) &= n^*(\bar{x}_t) + \xi_t(x) \\
\Rightarrow \xi_{t+1}(x) &= n_{t+1}(x) - n^*(\bar{x}_{t+1}) \\
&= n_{t+1}(x) - n^*(\bar{x}_t - c) \\
&= \int_{-L/2+ct}^{L/2+ct} k(x-y) R_0 g(f(n_t(y))) dy - \int_{-L/2}^{L/2} k(\bar{x}_t - \bar{y}_t) R_0 g(f(n^*(\bar{y}_t))) d\bar{y}_t \text{ using (3)} \\
&= \int_{-L/2+ct}^{L/2+ct} k(x-y) R_0 g(f(n_t(y))) dy - \int_{-L/2+ct}^{L/2+ct} k(x-ct-(y-ct)) R_0 g(f(n^*(\bar{y}_t))) d\bar{y}_t \\
&= \int_{-L/2+ct}^{L/2+ct} k(x-y) R_0 g(f(n_t(y))) dy - \int_{-L/2+ct}^{L/2+ct} k(x-y) R_0 g(f(n^*(\bar{y}_t))) d\bar{y}_t \\
&= \int_{-L/2+ct}^{L/2+ct} k(x-y) \left( R_0 g(f(n_t(y))) - R_0 g(f(n^*(\bar{y}_t))) \right) dy \\
&= \int_{-L/2+ct}^{L/2+ct} k(x-y) R_0 \left( g(f(n_t(y))) - g(f(n^*(\bar{y}_t))) \right) dy \\
\Rightarrow \xi_{t+1}(x) &= \int_{-L/2+ct}^{L/2+ct} k(x-y) R_0 g'(f(n^*(\bar{y}))) f'(n^*(\bar{y})) (n_t(y) - n^*(\bar{y}_t)) dy \\
&\quad \text{by linearizing around the traveling pulse} \\
\Rightarrow \xi_{t+1}(x) &= \int_{-L/2+ct}^{L/2+ct} k(x-y) R_0 g'(f(n^*(\bar{y}))) f'(n^*(\bar{y})) \xi_t(y) dy \\
\Rightarrow \xi_{t+1}(x) &= \int_{-L/2+ct}^{L/2+ct} k(x-y) R_0 g'(0) f'(0) \xi_t(y) dy \text{ if } n^*(\bar{x}) = 0 \text{ and } f(0) = 0
\end{aligned} \tag{4}$$

If we assume  $\xi_t(x) = \lambda^t u(x-ct)$  for some  $\lambda \in \mathbb{R}$  and  $u : [-L/2, L/2] \rightarrow \mathbb{R}$ , then the

perturbation grows in time if and only if  $\lambda > 1$ . Using Equation (4), we can rewrite  $\xi_{t+1}(x)$ ,

$$\begin{aligned} \lambda u(x - ct - c) &= R_0 g'(0) f'(0) \int_{-L/2+ct}^{L/2+ct} k(x - y) u(y - ct) dy \\ \Rightarrow \lambda u(\bar{x}) &= R_0 g'(0) f'(0) \int_{-L/2}^{L/2} k(\bar{x} + c - \bar{y}) u(\bar{y}) dy \end{aligned}$$

Define the integral operator

$$\psi_f(u)(x) = R_0 g'(0) f'(0) \int_{-L/2}^{L/2} k(x + c - y) u(y) dy.$$

Then the perturbation to the traveling pulse will satisfy

$$\psi_f(u)(x) = \lambda u(x) \quad (5)$$

$\lambda$  and  $u$  are thus an eigenvalue and eigenfunction of the functional operator  $\psi_f$ . The trivial traveling pulse is unstable when the dominant eigenvalue of  $\psi_f$  is greater than 1.

The biomass in the equilibrium traveling wave depends on the specific functional forms of the harvesting function  $g(n)$  and the recruitment function  $f(n)$ . However, the persistence of the population only depends on  $R_0$ ,  $g'(0)$  and  $f'(0)$ . In this paper, we only considered a proportional harvesting function, i.e. the amount of adults harvested obeyed  $g(n) = (1 - h)n$ . For this function,  $g'(0) = 1 - h$ . For the recruitment function we considered,  $f'(0) = 1$ .

**A.2 Separable dispersal kernels** It is not immediately obvious that the operator  $\psi$  will have any eigenfunctions. However, Jentzsch's theorem guarantees that there is an eigenfunction  $u$ , provided that the kernel  $k$  satisfies some properties [Zhou and Kot, 2011]. Finding the eigenfunctions and eigenvalues is in general a hard problem to solve. It becomes easier if the kernel  $k$  is separable, i.e., there are functions  $a_n, b_n$  such that  $k(x - y) = \sum_{n=1}^{\infty} a_n(x)b_n(y)$ . In that case, (5) becomes

$$\begin{aligned} \lambda u(x) &= R_0 g'(0) f'(0) \sum_{n=1}^{\infty} \left( a_n(x) \int_{-L/2}^{L/2} b_n(y - c) u(y) dy \right) \\ \Rightarrow \lambda \int_{-L/2}^{L/2} b_k(x - c) u(x) dx &= R_0 g'(0) f'(0) \sum_{n=1}^{\infty} \left( \int_{-L/2}^{L/2} b_n(x - c) u(x) dx \right) \left( \int_{-L/2}^{L/2} a_n(y) b_k(y - c) dy \right) \\ &\text{for any } k \\ \Rightarrow \lambda d_k &= R_0 g'(0) f'(0) \sum_{n=1}^{\infty} A_{nk} d_n \end{aligned} \quad (6)$$

where

$$A_{nk} = \int_{-L/2}^{L/2} a_n(x) b_k(x - c) dx \text{ and } d_k = \int_{-L/2}^{L/2} b_k(x - c) u(x) dx$$

Finding the eigenvalues of (5) then reduces to finding the eigenvalues of the matrix comprised of entires  $(A_{nk})_{n,k=1}^{\infty}$ .

To find the equilibrium biomass, we rewrite (3) using the separable kernel as in Latore et al. [1998]:

$$\begin{aligned} n^*(x) &= \int_{-L/2}^{L/2} k(x + c - y) R_0 g(f(n^*(y))) dy \\ &= \int_{-L/2}^{L/2} \left( \sum_{n=1}^{\infty} a_n(x) b_n(y - c) \right) R_0 g(f(n^*(y))) dy \\ &= \sum_{n=1}^{\infty} a_n(x) \int_{-L/2}^{L/2} b_n(y - c) R_0 g(f(n^*(y))) dy \end{aligned}$$

If we define  $m_n = \int_{-L/2}^{L/2} b_n(y - c) R_0 g(f(n^*(y))) dy$  then we find that

$$\begin{aligned} n^*(x) &= \sum_{n=1}^{\infty} m_n a_n(x) \text{ and} \\ m_n &= \int_{-L/2}^{L/2} b_n(y - c) R_0 g\left(f\left(\sum_{n=1}^{\infty} m_n a_n(y)\right)\right) dy \end{aligned} \quad (7)$$

The equations (7) allows us to find the  $m_n$  numerically and we then find the total equilibrium biomass by integrating  $n^*(x)$  over space.

**A.3 Gaussian dispersal kernel** The Gaussian dispersal kernel is given by

$$k(x - y) = \frac{1}{2\sqrt{D\pi}} e^{-\frac{(x-y)^2}{4D}},$$

where  $D$  is one half the variance of the kernel. This is a separable kernel with  $a_n(x) = b_n(x) = \frac{1}{\sqrt{2n!\sqrt{D\pi}}} e^{-x^2/4D} \left(\frac{x}{\sqrt{2D}}\right)^n$  [Latore et al., 1998].

As a first approximation to  $k$  we ignore all but the  $0^{th}$  terms for  $a_n$  and  $b_n$  so that Equation (6) becomes

$$\begin{aligned} \lambda d_0(c) &= R_0(1 - h) A_{00}(c) d_0(c) \\ \Rightarrow \lambda &= R_0(1 - h) A_{00}(c) \\ \text{where } A_{00}(c) &= 2\sqrt{2} \exp\left(\frac{-c^2}{8D}\right) \left[ \operatorname{erf}\left(\frac{L-c}{2\sqrt{2D}}\right) - \operatorname{erf}\left(\frac{-L-c}{2\sqrt{2D}}\right) \right] \end{aligned}$$

where  $\operatorname{erf}$  is the error function. The critical rate of environmental shift  $c^*$  and the critical harvesting rate  $h^*$  are those values of  $c$  and  $h$ , respectively, that make  $\lambda = 1$ .

**A.4 Sinusoidal dispersal kernel** The sinusoidal dispersal kernel is given by

$$k(x - y) = \begin{cases} \frac{w}{2} \cos(w(x - y)) & , \quad |x - y| \leq \frac{\pi}{2w} \\ 0 & , \quad |x - y| > \frac{\pi}{2w} \end{cases}$$

where  $L$  is the length of the patch and we assume  $\frac{\pi}{2w} > L, c < \frac{\pi}{2w} - L$ .

In this case,  $k(x - y) = \frac{w}{2} \cos(wx) \cos(w(y - c)) + \frac{w}{2} \sin(wx) \sin(w(y - c))$  so that  $A_{ij}$  and  $d_i$  can be found for  $i, j = 1, 2$  and (6) reduces to

$$\lambda^2 - \left( \frac{R_0(1-h)wL}{2} \cos(wc) \right) \lambda + \frac{R_0^2(1-h)^2}{16} (w^2 L^2 - \sin^2(wL)) = 0.$$

If we solve for  $\lambda$ , we find

$$\lambda = (1-h)R_0 \left[ \frac{wL \cos(wc)}{4} + \frac{1}{4} \sqrt{\sin^2(wL) - w^2 L^2 \sin^2(wc)} \right].$$

Zhou and Kot [2011] solve for the critical speed,  $c^*$ , at which the population will be driven extinct:

$$c^* = c^*(R_0) = \frac{1}{w} \cos^{-1} \left[ \frac{16 + R_0^2(1-h)^2(w^2 L^2 - \sin^2(wL))}{8R_0(1-h)wL} \right].$$

In our model, we can additionally solve for the critical harvesting rate,  $h^*$ , at which the population will be driven extinct:

$$h^* = 1 - \frac{1}{R_0} \cdot \frac{4wL}{w^2 L^2 - \sin^2(wL)} \left[ \cos(wc) - \sqrt{\cos^2(wc) - 1 + \frac{\sin^2(wL)}{w^2 L^2}} \right]$$

## A.5 Approximate critical harvesting proportions

We will use the following Taylor series to make approximations of the critical harvesting proportions under the two dispersal kernels:

$$\begin{aligned} \cos(x) &= 1 - \frac{x^2}{2} \\ \cos^2(x) &= 1 - x^2 \\ \sin^2(x) &= x^2 - \frac{x^4}{3} \\ \text{erf}(x) &= \frac{2}{\sqrt{\pi}} \left( x - \frac{x^3}{3} \right) \\ \exp(x) &= 1 + x + \frac{x^2}{2} \end{aligned}$$

For the Gaussian kernel we found

$$h^* = 1 - \frac{2\sqrt{2} \exp\left(\frac{c^2}{8D}\right)}{R_0 \left[ \text{erf}\left(\frac{L-c}{2\sqrt{2D}}\right) - \text{erf}\left(\frac{-L-c}{2\sqrt{2D}}\right) \right]} \quad (8)$$

Using the Taylor series and the fact that  $D = \frac{\sigma^2}{2}$  where  $\sigma^2$  is the variance of the exponential kernel,

$$\begin{aligned} h^* &\sim 1 - \frac{\sqrt{2\pi} \left( 1 + \frac{c^2}{8D} + \frac{c^4}{128D^2} \right)}{R_0 \sqrt{\pi} \left[ \frac{L-c}{2\sqrt{2D}} - \frac{(L-c)^3}{3(2\sqrt{2D})^3} - \frac{-L-c}{2\sqrt{2D}} + \frac{(-L-c)^3}{3(2\sqrt{2D})^3} \right]} \\ &= 1 - \frac{1}{R_0} \cdot \frac{3\sqrt{2\pi}}{8L} \frac{(32\sigma^4 + 8c^2\sigma^2 + c^4)}{\sigma(12\sigma^2 - (L^2 + 3c^2))} \end{aligned}$$

For the sinusoidal kernel we found

$$h^* = 1 - \frac{1}{R_0} \cdot \frac{4wL}{w^2L^2 - \sin^2(wL)} \left[ \cos(wc) - \sqrt{\cos^2(wc) - 1 + \frac{\sin^2(wL)}{w^2L^2}} \right] \quad (9)$$

Using the Taylor series and the fact that  $w = \frac{\sqrt{\frac{\pi^2}{4} - 2}}{\sigma}$  where  $\sigma^2$  is the variance of the sinusoidal kernel,

$$\begin{aligned} h^* &\sim 1 - \frac{1}{R_0} \cdot \frac{12wL}{w^4L^4} \left[ 1 - \frac{w^2c^2}{2} - \sqrt{1 - w^2c^2 - \frac{w^2L^2}{3}} \right] \\ &= 1 - \frac{1}{R_0} \cdot \frac{4\sqrt{3}}{L^3(\pi^2 - 8)^{3/2}} \cdot \sigma \left[ 8\sqrt{3}\sigma^2 - (\pi^2 - 8)\sqrt{3}c^2 - 4\sigma\sqrt{12\sigma^2 - (\pi^2 - 8)(3c^2 + L^2)} \right] \end{aligned}$$

In the case of both kernels, the critical harvesting proportion can be approximated by a function that looks like

$$h^* \sim 1 - \frac{1}{R_0} \cdot p(L)q(\sigma^2, c^2, L^2 + 3c^2) \quad (10)$$

where  $p(L)$  is a decreasing function of the length of the viable patch  $L$ .

## A.6 MPA fluctuations

After the simulations come to equilibrium, the fluctuations in total biomass per generation fluctuate more in MPAs that are larger and spaced farther apart than simulations in which the MPAs that are smaller and more closely spaced. The large MPAs have a slightly larger average population, however large MPAs here can induce fluctuations of biomass even in deterministic simulations. Thus we expect if reproduction was stochastic, large MPAs spaced far apart would be more likely to result in extinction of the population than more closely spaced, smaller MPAs.

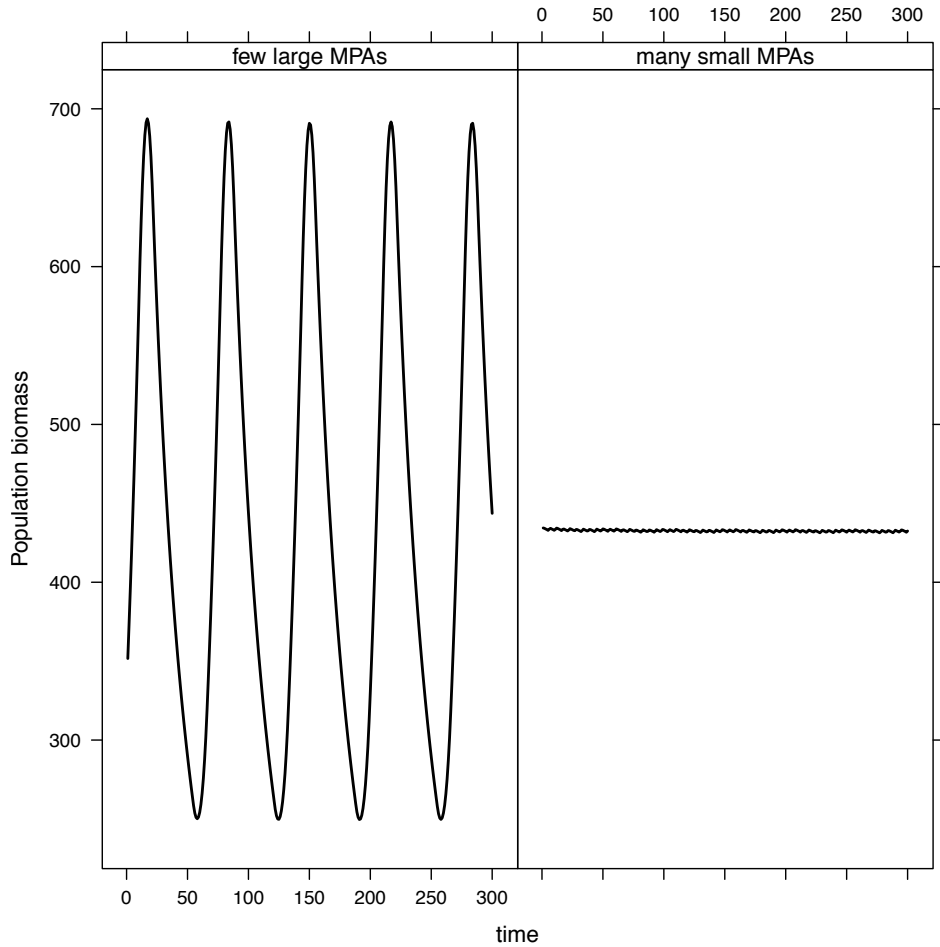


Figure 1: Total population biomass is on the y axis, and generation is on the x axis. These simulations were run with climate velocity = 0.1, and a proportional harvest rate = 0.08.

### A.7 Re-allocation of Effort

Spatial shifts of harvesters in response to MPA creation can affect sustainability of the system [Botsford et al., 2009]. We model the two extremes of response: either that harvesting pressure that occurred in now-MPAs is reallocated outside the reserves, or harvesting inside MPAs disappears from the system with the creation of MPAs and MPAs are effectively an effort control management technique. To reallocate effort we increased quota by 50% in outside of MPAs (see Kaplan and Botsford [2005] for similar approach).

We found no qualitative change in our results. Reallocation of effort was effectively like increasing the harvesting rate, and thus the critical harvest rate was lower than when effort was removed from the system.

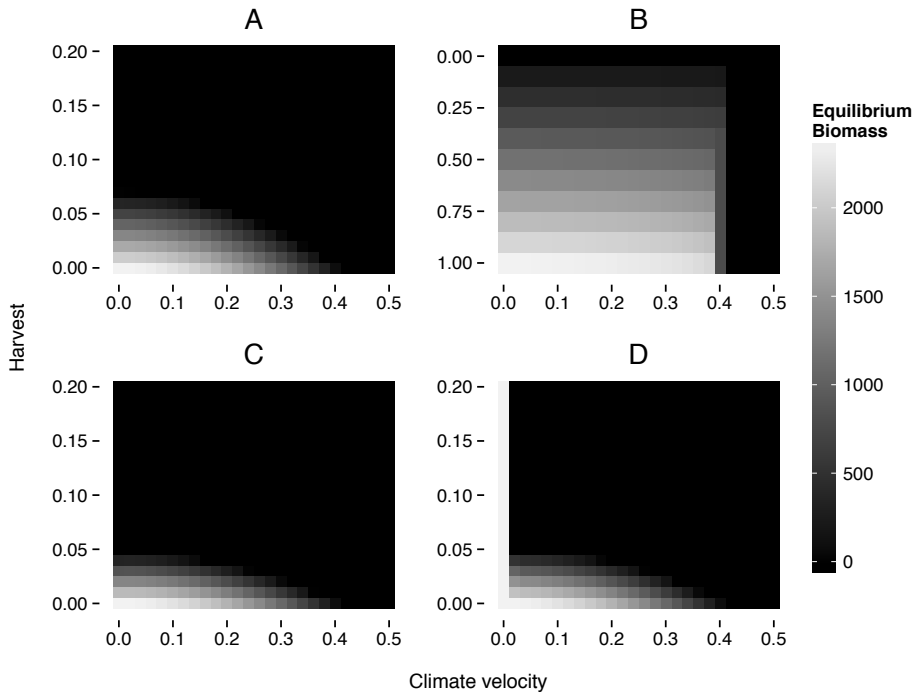


Figure 2: Climate velocity is on the x axis, harvest rate is on the y axis. These simulations were run with effort reallocated to areas outside of MPAs.

## References

Louis W. Botsford, Daniel R. Brumbaugh, Churchill Grimes, Julie B. Kellner, John Largier, Michael R. O'Farrell, Stephen Ralston, Elaine Soulard, and Vidar Wespestad. Connectivity, sustainability, and yield: bridging the gap between conventional fisheries management and marine protected areas. *Reviews in Fish Biology and Fisheries*, 19(1):69–95, 3 2009. ISSN 0960-3166. doi: 10.1007/s11160-008-9092-z.

David M. Kaplan and Louis W. Botsford. Effects of variability in spacing of coastal marine reserves on fisheries yield and sustainability. *Canadian Journal of Fisheries and Aquatic Sciences*, 62:905–912, 2005.

J. Latore, P. Gould, and A. M. Mortimer. Spatial dynamics and critical patch size of annual plant populations. *Journal of Theoretical Biology*, 190(3):277–285, 1998.

Ying Zhou and Mark Kot. Discrete-time growth-dispersal models with shifting species ranges. *Theoretical Ecology*, 4(1):13–25, 2 2011. ISSN 1874-1738. doi: 10.1007/s12080-010-0071-3.

```

# Make.R --> Wrapper script to run simulations
rm(list=ls())
require(plyr)
require(lattice)

# load parameters, functions
source("Parameters.R")
source("Functions.R")

# set up different parameter combinations for all simulations

sims <- data.frame(model =
  c("noThresh", "noThresh", "noThresh", "noThresh", "noThresh", "Thresh"),
  MPA = c("cons", "cons", "fish", "fish", "null", "null"),
  effort_allocate = c(NA, "yes", NA, "yes", NA, NA),
  stringsAsFactors=FALSE)

for(run in 1:nrow(sims)){
  # run analysis
  # choose threshold or no threshold
  model = sims$model[run] # "noThresh"; "Thresh"

  # if no threshold, choose MPA: "null", "cons", "fish"
  MPA = sims$MPA[run]
  # choose how effort should be allocated if MPAs present.
  effort_allocate = sims$effort_allocate[run]
  effort_allocate = ifelse(MPA!="null", effort_allocate, NA)

  # analysis
  timed <- system.time(
    if(model=="noThresh")
    {sapply(c("Parameters_nothresh.R", "Sim_noThresh.R"), source, .GlobalEnv)} else {
      if(model=="Thresh" & MPA == "null")
      {sapply(c("Parameters_thresh.R", "Sim_thresh.R"), source, .GlobalEnv)} else {
        warning("model needs to be 'noThresh' or 'Thresh', MPA needs to be 'null'")
      }
    }
  )
}

cat(paste("Time elapsed: ", round(timed[1]/3600,3), " hours\n", "Finished running a ", model, " simulation with ", MPA, " MPAs", " and effort re_allocate set to ", effort_allocate, ".\n", nrow(sims)-run, " simulations left to go...", sep=""))
}

#-----#
# Functions.R ---> defines reproduction, dispersal, and climate velocity functions used in simulations

#Laplace dispersal kernel
k<-function(x,y,b) return(1/2*b*exp(-b*abs(x-y)))

# dispersal matrix
d<-array(,c(w,w))
#dispersal probabilities to point i from every point j
for(i in 1:w) d[i,]=k(world[i],world,b)

```

```

#Beverton-Holt recruitment
f<-function(n,R0,K) return(R0*n/(1+(R0-1)/K*n))

#Standard error removing NAs
stderr <- function(x) sqrt(var(x,na.rm=TRUE)/length(na.omit(x)))

moveMPA <- function(MPA.current = MPA.current, displaced = displaced, mpa.yes=mpa.yes,
mpa.no=mpa.no, world){

##### Move MPAS
# move MPA forward by <displaced> amount
next_MPA = MPA.current[displaced:length(MPA.current)]
lost <- MPA.current[1:(displaced-1)]

# are there any MPAs in <next_MPA>?
#any(test[[i]]$next_MPA==1)
# IF FALSE, then need to figure out how many 0s were lost in
# move, and make sure to preserve interval of zeros == mpa.no,
# then fill in mpa.yes,mpa.no to length of world. But also this
# is only for when mpa.no exists on both sides of MPA_next. If
# exactly to the edge of one reserve is lost, should shift down
# to next if statement
if(any(next_MPA==1)==FALSE & any(lost==1)==TRUE){
  # these are the intervals that are left behind as world moves
  # forward
  lost <- MPA.current[1:(displaced-1)]
  # this is the last continuous chunk of numbers at the end of
  # <lost>
  length_last <- rep(tail(rle(lost)$value,1),
    tail(rle(lost)$lengths,1))
  # want to know how long <length_last> is so can make sure to
  # get correct interval
  L_int <- length(length_last)
  # how many more zeros do we need before we start with mpa.yes
  # again?
  zero_add <- sum(mpa.no==0) - L_int - sum(next_MPA==0)
  # this is what needs to be appended to <next_MPA>
  new_MPA <- c(rep(0,zero_add),
    rep(c(mpa.yes,mpa.no),
      length.out=length(world)))
}

else{
  # IF FALSE (there are some 1s) then we only care about the
  # last interval of the <next_MPA>, is that protected or not?
  last_step = tail(next_MPA,1)
  # IF <last_step>==1
  if(last_step ==1){
    #then how many 1s are at the end of the <next_MPA> section?
    end_step = rep(tail(rle(next_MPA)$value,1),
      tail(rle(next_MPA)$lengths,1))
    # number of 1s at very end of lost interval
    # length of <end_step>
  }
}

```

```

end_int = length(end_step)
# need to prepend sum(mpa.yes==1) - <end_step> to beginning
prepend = rep(1, (sum(mpa.yes==1) - end_int))
# and then fill out with mpa.no,mpa.yes for length of world
fillOut <- rep(c(mpa.no, mpa.yes),
               length = (length(world) - length(prepend)))
}else{
# IF <last_step>==0
end_step = rep(tail(rle(next_MPA)$value,1),
               tail(rle(next_MPA)$lengths,1))
# number of 0s at very end of lost interval
# length of <end_step>
end_int = length(end_step)
# need to prepend sum(mpa.no==0) - <end_step> to beginning
prepend = rep(0, (sum(mpa.no==0) - end_int))
# and then fill out with mpa.no,mpa.yes for length of world
fillOut <- rep(c(mpa.yes, mpa.no),
               length = (length(world) ))
}
new_MPA = c(prepend,fillOut)
}

MPA_finish = c(next_MPA,new_MPA)
MPA_finish = MPA_finish[1:length(world)]
# reduce to just the size of the world

return(MPA_finish)
}

m <- function(n, s, Fthresh = NA, Fharv = NA, mpa.yes = NA,
              mpa.no = NA, MPA.current=NA,effort_re_allocate=NA){
# steps
# 1. Harvest (check for thresholds, harvesting, MPA coverage)
# 2. Patch moves (and MPAs are adjusted)
# 3. Individuals outside patch die
# 4. Individuals still alive (ie inside the patch) reproduce

# harvesting occurs first - check to see how should
# re-allocate effort

if(!is.na(effort_re_allocate) & !is.na(Fharv)){ # harvesting non-zero and effort
reallocate
    #total_catch = sum(n)*Fharv
    total_catch = sum(n)*Fharv * 1.5 # increasing effort by 50% to account for effort-
reallocation
    available_total_pop = sum(n[which(MPA.current==0)])
    # pop with no MPA coverage
    available_fish = rep(0,length(n))
    available_fish[MPA.current==0] <-
        n[MPA.current==0]/available_total_pop
        # available_total_pop
    # proportion at each point
    catch_in_space <- total_catch*available_fish
    # allocate catch
}

```

```

    next_gen = n - catch_in_space
    next_gen[next_gen < 0] = 0
} else{
  if(!is.na(Fthresh)) { # if thresholds
    next_gen = ifelse(n < Fthresh,
                      n, n - (n - Fthresh) * Fharv)
  }
  if(!is.na(Fharv) & is.na(Fthresh)) {
    # if harvesting, no thresholds
    next_gen = n*(1-Fharv)
  }
  if(is.na(Fharv) & is.na(Fthresh)) {next_gen = n}
  # if no harvesting of any kind

  # but put fish back if places that were harvested were in
  # the MPA
  next_gen[MPA.current == 1] <- n[MPA.current == 1]
}

# move the patch
# calculate how far the patch will move through the population
# (if speed !=0)
displaced = ifelse(s>0,s/step_size,1)

# assign population that will still be inside the patch to
# moved patch
next_n = next_gen[displaced:length(next_gen)]

# fill in newly existing patch with 0s
next_n = c(next_n,rep(0,length.out=(displaced-1)))

# move MPAs?
if(s > 0){MPA_finish = moveMPA(MPA.current, displaced,
                                 mpa.yes,mpa.no,world)}else{MPA_finish= MPA.current}

# let patch reproduce
next_patch = vector(mode="numeric",length(world))

# keep individuals still in patch + those now in it due to
# move
next_patch[1:length(patch)] = next_n[1:length(patch)]

babies = next_patch*f_ind
n2 = babies %*% d *step_size
n2 = sapply(n2,f,R0,K)

MPA = MPA_finish
return(list(n2,MPA)) # removed a mysterious 'harv' from here
}

# wrapper function to run simulation for 6000 generations and save outcome from 2000
# additional generations to take average
longRun <- function(s, mpa.yes, mpa.no, Fthresh, Fharv, init,

```

```

MPA.start, generations_total, generations_av,
effort_re_allocate=effort_allocate){
MPA.current <- MPA.start
burn_in <- generations_total - generations_av
for(t in 1:(burn_in)){
  output = m(n=init, s = s, Fthresh=Fthresh,Fharv=Fharv,
  mpa.yes = mpa.yes, mpa.no = mpa.no,
  MPA.current = MPA.current, effort_re_allocate=effort_allocate)
  init= output[[1]]
  MPA.current = output[[2]]
}
# make dataframe for simulation average
pop <- rep(0,generations_av)
for(keep in 1:generations_av){
  output = m(n=init, s = s, Fthresh=Fthresh,Fharv=Fharv,
  mpa.yes = mpa.yes, mpa.no = mpa.no,
  MPA.current = MPA.current, effort_re_allocate = effort_allocate)
  init = output[[1]]
  MPA.current = output[[2]]
  pop[keep] = sum(output[[1]])
}
# take mean for equil_abundance
equil.pop = mean(pop)
equil.sd = sd(pop)

return(list(equil.pop,equil.sd))
}

# to introduce population to empty landscape, harvesting before
# adding speed treatment

# wrapper function to initialize the population, only returns results from final generation
startUp <- function(s, mpa.yes, mpa.no, Fthresh, Fharv, init,
  MPA.start, burn_in,effort_re_allocate=effort_allocate){
  MPA.current <- MPA.start
  for(t in 1:(burn_in)){
    output = m(n=init, s = s, Fthresh=Fthresh,Fharv=Fharv,
    mpa.yes = mpa.yes, mpa.no = mpa.no,
    MPA.current = MPA.current,
    effort_re_allocate=effort_allocate)
    init= output[[1]]
    MPA.current = output[[2]]
  }
  return(list(init,MPA.current))
}
#-----
# Parameters.R
#####
## Parameters & Building Structures ##
#####

```

```

step_size=0.01 #distance between points in space
b=.5 #parameter for Laplace dispersal kernel
R0=5 #growth parameter for recruitment
K=100 #carrying capacity parameter for juvenile density dependence
threshold = 0.001 #difference between generation populations.
burn_in = 2000 # number of generations to run simulations before checking for equilibrium
conditions
speeds = seq(0,.5,by=0.02)
harvests = seq(0,.2,by=0.01)
f_ind = 1 #per capita reproductive rate
generations_total = 8000
generations_av = 2000

patch = seq(0,1,by=step_size)
world = seq(-.51,4.5, by = step_size) # to run the MPA versions, world has to be at least
400 steps (max distance between MPAs in "cons" run)
w = length(world)

cons.yes = rep(1,4*b/step_size)
cons.no = rep(0,8*b/step_size)
fish.yes = rep(1,floor((1/3*b)/step_size)) # had to round because not complete step size.
Rounded down.
fish.no = rep(0,floor((2/3*b)/step_size))

null.yes = rep(0,length(world))
null.no = rep(0, length(world))

move_window = 100
#-----
# Parameters_nothresh.R
# parameters for no-threshold simulations (just proportional harvesting)

# build dataframes
summaries <- data.frame(
  Equil.pop = rep(NA,length=length(speeds)*length(harvests)),
  Equil.sd = rep(NA,length=length(speeds)*length(harvests)),
  speed = rep(NA,length=length(speeds)*length(harvests)),
  harvest = rep(NA,length=length(speeds)*length(harvests)),
  thresh = rep(NA,length=length(speeds)*length(harvests))
)

# index for row number
rownumber <- matrix(seq(1:(length(harvests)*length(speeds))),ncol=length(speeds))
#-----
# Parameters_thresh.R
# parameters for threshold simulations (no proportional harvesting)
harvests = 1
thresholds = seq(0,1,by=0.1)

# build dataframes
summaries <- data.frame(
  Equil.pop = rep(NA,length=length(speeds)*length(thresholds)),
  Equil.sd = rep(NA, length=length(speeds)*length(thresholds)),

```

```

speed = rep(NA,length=length(speeds)*length(thresholds)),
harvest = rep(NA,length=length(speeds)*length(thresholds)),
thresh=rep(NA,length=length(speeds)*length(thresholds)))

# index for row number
rownumber <- matrix(seq(1:(length(thresholds)*length(speeds))),ncol=length(speeds))
#-----#
# Sim_noThresh.R
# runs simulations in which there is no threshold management, MPAs are possible

# set MPAs
if(MPA=="cons") {mpa.yes=cons.yes; mpa.no=cons.no} else {
  if(MPA=="fish") {mpa.yes=fish.yes; mpa.no=fish.no} else {
    if(MPA=="null") {mpa.yes=null.yes; mpa.no=null.no} else{
      if(exists("MPA")) warning(paste("MPA needs to be 'cons', 'fish', or
'null'.",sep=""))
    }
  }
}

# initializing the population with no pressure (no harvesting, no climate)
init<-rep(0,w) # rows are world, columns are time
init[which(patch==0.55)]=50
MPA.start = rep(c(mpa.yes,mpa.no),length.out=length(world))

output <- startUp(s=0,mpa.yes=mpa.yes,mpa.no=mpa.no,burn_in=burn_in, Fharv=NA,
Fthresh=NA, init=init, MPA.start = MPA.start, effort_re_allocate=NA)
init.s <- output[[1]]
MPA.start <- output[[2]]

for(q in 1:length(speeds)){
  for(j in 1:length(harvests)){
    # adding harvesting
    output <-
startUp(s=0,mpa.yes=mpa.yes,mpa.no=mpa.no,burn_in=burn_in,Fharv=harvests[j],Fthresh=NA,
init=init.s, MPA.start = MPA.start, effort_re_allocate=effort_allocate)
    init.h <- output[[1]]
    MPA.start <- output[[2]]

    # adding speed
    output <- longRun(s=speeds[q], mpa.yes=mpa.yes, mpa.no=mpa.no, Fthresh=NA,
Fharv=harvests[j], init = init.h, MPA.start = MPA.start,
generations_total=generations_total, generations_av=generations_av,
effort_re_allocate=effort_allocate)

    # save output
    pop = output[[1]]
    pop.sd = output[[2]]
    summaries[rownumber[j,q],] <- c(pop, pop.sd, speeds[q], harvests[j],
ifelse(exists("Fthresh"), Fthresh,NA))
  }
}

```

```

write.csv(summaries,file = paste("Data/
MPA",MPA,"_",effort_allocate,"_",Sys.Date(),".csv",sep=""))
#-----#
# Sim_thresh.R
# runs simulations in which there is threshold management, MPAs are not possible

# initializing the population with no pressure (no harvesting, no climate)
init<-rep(0,w) # rows are world, columns are time
init[which(patch==0.55)]=50
MPA.start = rep(c(mpa.yes,mpa.no),length.out=length(world))

output <- startUp(s=0,mpa.yes=mpa.yes,mpa.no=mpa.no,burn_in=burn_in, Fharv=NA,
Fthresh=NA, init=init, MPA.start = MPA.start)
init.s <- output[[1]]
MPA.start <- output[[2]]

for(q in 1:length(speeds)){
  for(j in 1:length(thresholds)){
    # adding harvesting
    output <-
startUp(s=0,mpa.yes=mpa.yes,mpa.no=mpa.no,burn_in=burn_in,Fharv=1,Fthresh=thresholds[j],
init=init.s, MPA.start = MPA.start, effort_re_allocate=effort_allocate)
    init.h <- output[[1]]
    MPA.start <- output[[2]]Fharv=1

    # adding speed
    output <- longRun(s=speeds[q], mpa.yes=mpa.yes, mpa.no=mpa.no,
Fthresh=thresholds[j], Fharv=1, init = init.h, MPA.start = MPA.start,
generations_total=generations_total, generations_av=generations_av,
effort_re_allocate=effort_allocate)

    # save output
    pop = output[[1]]
    pop.sd = output[[2]]
    summaries[rownumber[j,q],] <- c(pop, pop.sd, speeds[q], 1,
ifelse(exists("thresholds"), thresholds[j],NA))
  }
}

write.csv(summaries,file = paste("Data/Thresh_",Sys.Date(),".csv",sep=""))
#-----#

```